

Bi-directional Momentum-based Haptic Feedback and Control System for Dexterous Telemanipulation

Haoyang Wang*, Haoran Guo*, He Bai*, *Member, IEEE*, ^Zhengxiong Li, *Member, IEEE*, Lingfeng Tao*, *Member, IEEE*

Abstract — Haptic feedback is essential for dexterous telemanipulation that enables operators to control robotic hands remotely with high skill and precision, mimicking a human hand's natural movement and sensation. However, current haptic methods for dexterous telemanipulation cannot support torque feedback, resulting in object rotation and rolling mismatches. The operator must make tedious adjustments in these tasks, leading to delays, reduced situational awareness, and suboptimal task performance. This work presents a Bi-directional Momentum-based Haptic Feedback and Control (Bi-Hap) system for real-time dexterous telemanipulation. Bi-Hap integrates multi-modal sensors to extract human interactive information with the object and share it with the robot's learning-based controller. A Field-Oriented Control (FOC) algorithm is developed to enable the integrated brushless active momentum wheel to generate precise torque and vibrative feedback, bridging the gap between human intent and robotic actions. Different feedback strategies are designed for varying error states to align with the operator's intuition. Extensive experiments with human subjects using a virtual Shadow Dexterous Hand demonstrate the effectiveness of Bi-Hap in enhancing task performance and user confidence. Bi-Hap achieved real-time feedback capability with low command following latency (delay<0.025s) and highly accurate torque feedback (RMSE<0.010 N · m).

I. INTRODUCTION

Dexterous telemanipulation [1], which facilitates the remote execution of complex tasks through robotic systems, has become increasingly essential in critical domains such as medical surgery [2], hazardous material handling [3], and space exploration [4]. Achieving effectiveness in these applications requires precise, continuous control of a robotic hand by a human operator, with success depending on the seamless integration of control and feedback mechanisms for sophisticated object interactions. However, significant challenges persist: 1) the indirect nature of remote operation, leading to increased operator burden and reduced situational awareness; 2) the force feedback devices currently applied in dexterous telemanipulation do not effectively convey torque, requiring the operator to make laborious adjustments; 3) the torque output is difficult to control due to the weight and speed of the momentum wheels.

In current dexterous telemanipulation systems, haptic feedback methods primarily utilize devices such as cutaneous displays [5], vibrotactile motor [6], and haptic gloves [7], which are designed to map the fingertip forces experienced by the robotic hand onto the human operator's hand. These

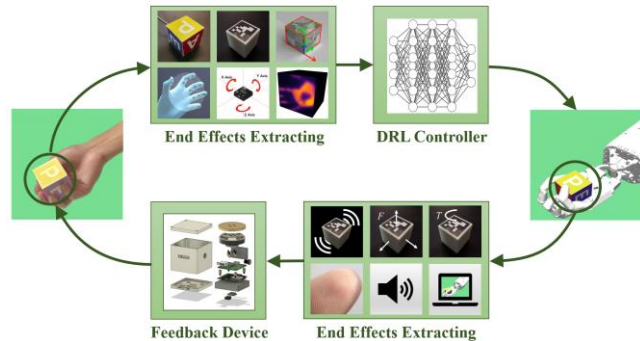


Fig.1. The data flows in the proposed Bi-Hap system provides bi-directional feedback and control that not only utilize the end-effect-oriented DRL-based control from the human to the robot, but also recreate the seamless manipulation feeling with the torque and vibrative feedback from the robot back to the human.

techniques either restrict the range of motion of the operator's hand joints or apply external force to deform the skin to simulate the robotic hand's interaction forces. While these approaches aim to correlate robotic hand forces with human sensory feedback directly, they are constrained by size and technological limitations, with each finger typically supporting force feedback in only one or two degrees of freedom. This limitation is insufficient for generating the torque feedback necessary for object rotation, a critical aspect in many applications. Consequently, operators must make challenging adjustments when wearing the devices based on feedback that may be indirect or counter-intuitive, impairing task efficiency and potentially compromising safety.

Momentum-based haptic devices have shown great potential in the domain of haptic feedback, offering an innovative approach to simulating torque and vibrations in interactive systems. For instance, HapticWhirl [8] generates a range of haptic effects using a flywheel system that provides torque feedback to enable realistic replicating impact effects, such as the feedback experienced when holding a racket and striking a ball. MetamorphX [9], utilizing Control Moment Gyroscopes (CMGs), offers ungrounded, 3 Degrees of Freedom (DoF) feedback that simulates inertia and viscosity in VR environments. Participants highlighted enhanced realism and enjoyment from the moment feedback and synchronized visuals. These examples illustrate the importance of torque feedback, as it improves task performance and increases user confidence by narrowing the gap between human and robot interaction. Unlike conventional haptic devices that depend on motors or actuators fixed to the ground for direct force application, momentum-based systems generate inertial forces using spinning masses like momentum wheels. This allows for a compact and portable design while delivering rich haptic

This work is supported by NSF #2426269 and #2426470.

*H. Wang, H. Bai and L. Tao are with the Oklahoma State University, 563 Engineering North, Stillwater, OK, 74078, USA (e-mail: haoyang.wang; haoran.guo; he.bai; lingfeng.tao@oksate.edu).

^Z. Li is with the University of Colorado Denver, I Department of Computer Science and Engineering, 1380 Lawrence St. Center, LW-834, Denver, CO 80217, USA (e-mail: zhengxiong.li@ucdenver.edu).

feedback, including torque, impact simulation, and both low-frequency and high-amplitude vibrations [8, 9]. Despite these advantages, momentum-based haptic devices are not studied in dexterous telemanipulation. One of the primary difficulties is due to the difficulty in system integration and controlling these systems, which is complicated by the inherent inertia of spinning masses, resulting in latency in feedback, which is critical in dynamic telemanipulation.

This work develops a Bi-directional Momentum-based Haptic Feedback and Control System (Bi-Hap) that extracts end-effect features for the learning-based robot controller and delivers real-time, low-latency torque and vibration feedback to the human operator during telemanipulation. We integrate the EFOLD [9] learning-based telemanipulation from our previous work, which uses a DRL controller to control the robot to recreate the human-object interactions—such as movement, force, and deformation to achieve minimal error and real-time control. Using an active momentum wheel, Bi-Hap provides precise and responsive feedback, capturing the angular difference between the manipulated object and the target. Feedback methods are categorized into internal and external approaches: internal feedback integrates the mechanism directly within the object, such as embedding sensors and actuators inside the system. In contrast, external feedback uses visual or auditory cues to inform the operator. Building upon this framework, several adaptive feedback strategies are introduced, tailoring the feedback’s intensity and type to varying operational conditions, ensuring intuitive control and effective feedback. The contributions of this work are summarized as follows:

- 1) Designed a novel Bi-Hap system that enables real-time control of the robotic hand and provides low-latency, high-precision torque and vibration feedback.
- 2) Developed multiple feedback strategies for different telemanipulation conditions to adapt to human feeling and improve the accuracy of manipulation.
- 3) Tested Bi-Hap system with real human subjects in telemanipulation tasks using a virtual Shadow Dexterous hand and used the manipulated object as a joystick to play the game, highlighting its versatility and potential for broader applications.

II. RELATED WORK

A. Telemanipulation with Haptic Feedback

Haptic feedback has established itself as an essential tool for enhancing robotic telemanipulation, significantly improving operator performance in applications such as grasping [11], assembly [12], and surgical robotics [13]. The feedback provided to operators can be classified into cutaneous and kinesthetic stimulation. Cutaneous stimuli [14], also known as tactile feedback, are detected by skin receptors, allowing users to perceive object properties like shape, edges, temperature, and texture. Conversely, kinesthetic stimuli [15] originate from muscles, joints, and skin, providing critical information about body positioning, velocity, and the forces and torques applied.

Cutaneous feedback has recently attracted considerable attention for its compact, comfortable, and cost-effective design. For example, [16] introduces a skin feedback system for surgical robots, which provides cutaneous feedback through fingertip contact deformation and vibration. This system utilizes BioTac tactile sensors and custom skin displays connected to the master controller, with contact

deformations and vibrations directly mapped to the motors of the cutaneous device using a model-free algorithm based on look-up tables. Recent advances in manufacturing have facilitated the development of more refined feedback systems. For instance, [17] presents a novel teleoperation system that converts proximity-sensing data from the slave system into tactile feedback for the user. This is achieved through a 4×4 resolution tactile display that enhances centering accuracy while ensuring acceptable completion times. However, since humans are accustomed to full tactile feedback, which includes both force and torque, the current methods that only provide force feedback still face challenges in terms of insufficient user perception.

B. Momentum-based Haptic Feedback Device

Momentum-based haptic feedback devices, with their ungrounded design and ability to provide torque feedback within objects, are increasingly applied in virtual reality [9, 18, 19], healthcare [20, 21, 22], and human-computer interaction [9, 23, 24]. These devices commonly use momentum wheels, which generate gyroscopic effects when rotated, translating into force and torque feedback [25]. In [26], the GyroCube, a mobile torque-feedback device, is introduced, with experiments evaluating how the human hand perceives the generated forces. Similarly, [20] introduces the GyroPack, a wearable robotic gyroscopic actuator, and explores its influence on balance and walking tasks. Results indicate that gyroscopic actuators can impact balance and gait kinematics. Recent advancements include [9], which proposes MetamorphX, which employs Control Moment Gyroscopes (CMGs) to create ungrounded, 3-degrees-of-freedom moment feedback. By applying impedance control, MetamorphX adjusts motion inertia and viscosity to reflect the characteristics of a grasped object. User experiments, such as manipulating a fan and simulating interactions in a virtual environment, demonstrate the device’s ability to represent varying levels of inertia and viscosity, enhancing the immersive VR experience. However, due to the inherent inertia of the rotating masses, controlling these systems becomes complex, leading to unstable feedback in dynamic applications. As a result, they are currently not adopted in dexterous telemanipulation systems.

III. BI-DIRECTIONAL HAPTIC FEEDBACK AND CONTROL SYSTEM

In this section, we present the design of the Bi-Hap haptic feedback and control system, covering its hardware, working principle, and feedback strategy.

A. Hardware Implementation

The Bi-Hap system uses a modular design that can adapt to different telemanipulation tasks while maintaining a compact form that can adapt to varying sizes of human hands. Fig. 2 shows a block diagram of the system architecture, illustrating the architecture of the Bi-Hap system. The main modules of the system are as follows:

Torque Generating Module: The core module of the Bi-Hap hardware is a gimbal Brushless Direct Current (BLDC) motor and flywheel disk. The gimbal motor’s flat package design allows for greater rotational inertia with lighter weight. The total weight of the rotating disk and the motor’s rotating body is 128 g, with a diameter of 55 mm for the flywheel disk, and the inertia is $4.8 \times 10^{-5} \text{ kg} \cdot \text{m}^2$. We used an ESP32 Module to control the motor, and its wireless communication capability makes motor control easier. Using User Datagram

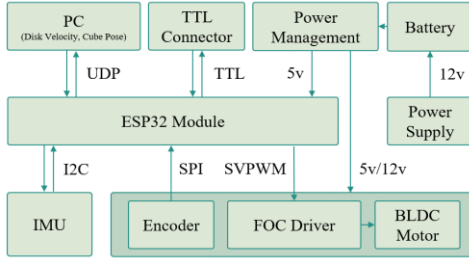


Fig. 2. Block diagram of the system showing the mechatronic components and relevant connections.

Protocol (UDP), the PC sends motor commands efficiently and receives motor feedback. Additionally, we developed a TTL connector for wired communication with the PC, which facilitates program uploading and debugging. Fig. 2 shows a block diagram of the system architecture, illustrating the architecture of the Bi-Hap device. To address the unstable torque output issue due to the rotating mass's inherent inertia, we implemented a closed-loop control program based on SimpleFOC [27], running on the ESP32. SimpleFOC is an open-source Arduino library that implements the Field Oriented Control (FOC) [28] algorithm for BLDC and stepper motors. FOC enables precise torque and speed regulation by aligning motor current with magnetic flux, resulting in smoother and more efficient operation. A key advantage of FOC is its ability to deliver high torque at low speeds, making it ideal for applications requiring accurate and stable motor control.

Data Acquisition Module: The device also includes a 14-bit resolution digital magnetic encoder AS5047, which communicates with the ESP32 via SPI, ensuring precise positional data is captured. An Inertial Measurement Unit (IMU) GY-95T measured the device's attitude. The GY-95T sends information to the microcontroller at 200 Hz, which includes angle data obtained through a data fusion algorithm that processes readings from the gyroscope, accelerometer, and magnetometer sensors.

Power Management Module: The system features power management, which regulates the 12V input from a battery or power supply, distributing it as needed to different components. An onboard 12V battery is integrated to provide the necessary energy. The gimbal BLDC motor operates on a 12 V supply, whereas the other electronics function at 5 V. The DC power interface can charge the battery or directly supply power to various modules, providing power support for extended use. A simple switch allows easy power control, making the device user-friendly and efficient.

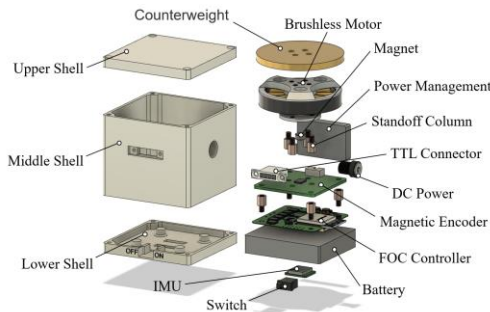


Fig. 3. Exploded view of a Bi-Hap system.

Shell Module: The casing component is essential not only to protect the mechanical and electronic device but also to be adaptable for different human users and manipulation tasks. Thanks to the modular design of the whole system, the inner components are nearly square, making it easy to fit in a common shell shape, such as a cube, sphere, or column. In this work, the shape of the Bi-Hap system is tested in a cube shell with a side length of 60 mm.

An exploded view of a Bi-Hap system is shown in Fig. 3. With the shell, the total weight of the Bi-Hap system is 320 g. Except for mechanical and electronic parts such as the motor and circuit board, all the casing components, including a three-layered shell structure consisting of upper, middle, and lower sections, were fabricated with PLA+ material using a 3D printer (Bamboo P1).

B. Working Principle

The law of conservation of angular momentum states that in the absence of external torque, the total angular momentum of a system remains constant. When a motor accelerates a flywheel, it increases its angular momentum. An equal and opposite angular momentum is generated in the motor or its supporting structure to conserve total angular momentum. The torque resulting from this change in angular momentum is calculated as:

$$\tau = -I_f \cdot \frac{d\omega_f}{dt} \quad (1)$$

where τ represents the counteracting torque on the motor or its supporting structure, I_f is the moment of inertia of the flywheel, and $\frac{d\omega_f}{dt}$ is the rate of change of the flywheel's angular velocity.

Our system regulates the flywheel's rotational speed using a discrete Proportional Integral Derivative (PID) controller [29]. The PID controller adjusts the motor voltage based on the error between the desired and actual angular velocities. The control input at the discrete time step k , denoted as $u(k)$:

$$u(k) = K_p e(k) + K_i \sum_{i=0}^k e(i) \Delta t + K_d \frac{e(k) - e(k-1)}{\Delta t} \quad (2)$$

where $u(k)$ is the control output at discrete time step k represents the voltage applied by the controller. The error $e(k)$ is the difference between the desired and actual angular velocity of the flywheel and $e(k-1)$ is the error at the previous moment. K_p, K_i and K_d are proportional gain, integral gain, and derivative gain. The sampling time interval Δt is the time between discrete control steps. By controlling the motor voltage using the discrete PID controller, we can regulate the flywheel's angular velocity to generate the desired feedback torque for the haptic device.

To make the interaction between the Bi-Hap system and the human operator more intuitive. We use an improved impedance control [30] to calculate the feedback strength. This control method adjusts the torque feedback response characteristics to the external environment during task execution, simulating a spring-damper system behavior. The calculation of the target torque value is calculated as:

$$\tau_d = K_{rot}(\theta_d - \theta) + B_{rot}(\dot{\theta}_d - \dot{\theta}) + M_{rot}(\ddot{\theta}_d - \ddot{\theta}) \quad (3)$$

where τ_d is the desired torque, θ is the current rotation angle, θ_d is the desired rotation angle, $\dot{\theta}$ is the current angular velocity, $\dot{\theta}_d$ is the desired angular velocity, $\ddot{\theta}$ is the current angular acceleration, $\ddot{\theta}_d$ is the desired angular

acceleration, K_{rot} is the rotational stiffness coefficient, B_{rot} is the rotational damping coefficient, and M_{rot} is the rotational inertia coefficient. This equation describes how the robot adjusts its response to external forces by modifying virtual mass, damping, and stiffness to achieve the desired compliance and stability during control. To prevent flywheel speed saturation, the target torque adjusts the output mode rather than being directly applied. When the flywheel is unsaturated, torque is applied normally. If saturated, the torque magnitude is converted into a vibration amplitude for output, which is calculated as:

$$\tau_{out} = A\tau_d \sin(\omega t) \quad (4)$$

Where τ_{out} represents the final output signal, which is the torque feedback provided to the operators. A is the maximum amplitude of the vibration, ω is the angular frequency of the vibration, and t is the time variable.

C. Feedback Strategy

In our telemanipulation setup, human operators need to manipulate the Bi-Hap system, which sends end-effect information for the robot to track and provide haptic feedback to the human. As mentioned in the hardware implementation section, we selected IMU as the built-in sensor to extract the Bi-Hap rotational position. As for the feedback forms, we employed torque, vibration, visual and auditory feedback as the feedback methods to guide the human operator. Based on the defined feedback forms, we identified the following manipulation scenarios and designed the corresponding feedback strategies:

Normal Manipulation: In this case, feedback is provided solely through visual cues. This strategy suits situations where the object is neither too close nor too far from the target angle. Visual feedback alone can effectively convey the difference between the current angle and the target to the human operator, and excessive feedback may unnecessarily increase the operator's cognitive load.

Target Position Reached: Audio feedback and visual cues will notify the human operator when the target angle is reached. This includes a short, sharp "ding" sound and a turning green target display. In this case, torque feedback is unnecessary as it may cause the manipulated object to deviate from the target angle.

Target Position Overshot: Torque and visual feedback are provided in this scenario. Since human precision is limited, overshooting the target is common. The Bi-Hap system generates torque in the direction of the target to prompt the human operator to make the necessary adjustments.

Far from Target Position: In this scenario, both torque and visual feedback are used. If the target angle changes rapidly and the operator continues rotating away from it, the Bi-Hap system will occasionally apply torque towards the target to indicate that a major correction is needed. Feedback is only activated if the operator remains in the deviation area for more than 3 seconds, based on user feedback, to avoid overwhelming the operator with too frequent corrections.

Unsafe Movements: Due to current technological limitations, it is difficult for the robotic hand to achieve the same level of dexterity as a human hand, leading to unsafe rotations or displacements of the object. When the object's position moves outside of a specific range on the robot's hand—either due to the object being stuck or falling off—visual, auditory, and vibration feedback are provided simultaneously to alert the operator to take corrective action.

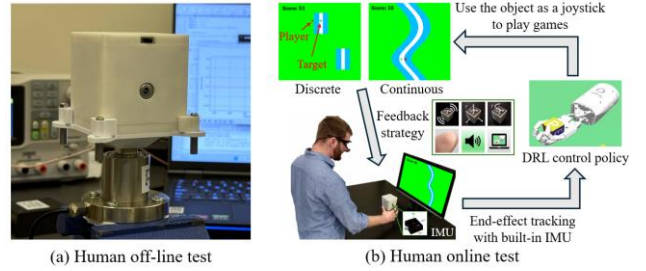


Fig. 4. (a) Human off-line and (b) Human online experiments. The white area in the figure represents the target region, and points are awarded when the red dot enters this area, corresponding to Target Position Reached. Exceeding the boundary of the white area corresponds to Target Position Overshot. The blue area serves as a warning zone, reminding the operator that adjustments are needed, corresponding to Normal Manipulation. The green area represents the forbidden zone, corresponding to Far From Target Position.

IV. EXPERIMENTS DESIGN AND EVALUATION METRICS

A. Experimental Setup and Task Design

To comprehensively evaluate the performance of the Bi-Hap system, we divided the testing into two categories:

Human offline: The human offline tests utilized traditional control theory methods [31] such as sinusoidal and square wave tracking analysis to objectively measure the device's torque feedback performance. A torque testing platform was constructed, as shown in Figure 4, equipped with a ZNNT-2NM torque sensor and 3D-printed fixtures. This sensor features a sampling frequency of 500Hz, a measurement range of 0-2NM, and a repeatability accuracy of 0.1%. It communicates with the host computer via RS-485 to accurately capture the torque the device generates. The PID control parameters used throughout all experiments, as mentioned in section III, are $K_p = 0.2$, $K_i = 20$ and $K_d = 0$.

Human online: The human online tests aimed to simulate real-world scenarios and evaluate overall system performance during telemanipulation tasks. These tests included discrete angle and continuous angle tasks, following the OSU IRB protocol. We use the Shadow Hand environments from the OpenAI GYM Robotics platform [32], running on the MuJoCo physics simulator [33]. As shown in Figure 4, the human operator uses the Bi-Hap system to control a robotic hand and rotate a block around the Z-axis to reach a target orientation. In the discrete angle task, the operator rotates the block to specific angles and holds each position briefly, guided by the Bi-Hap system. In the continuous angle task, the operator adjusts the block to match the rotation of a continuously rotating target. Additionally, we introduced a gaming environment where the Bi-Hap system acts as a feedback-enabled game controller, mapping the block's angle to a target point on the screen. Performance is measured by how often the operator successfully moves the on-screen dot to the target, comparing trials with and without Bi-Hap control. In all tasks, the end-effector feature, defined as the block's rotation angle φ around the Z-axis, is measured by the IMU embedded in the Bi-Hap system. The impedance control parameters used throughout all experiments, as mentioned in section III, are $K_{rot} = 2.5$, $B_{rot} = 1$ and $M_{rot} = 0$.

To the best of the authors' knowledge, no torque feedback devices in dexterous telemanipulation applications can serve as a baseline comparison. The only comparable approach is MetamorphX [9], which uses a torque feedback device held in hand. However, directly comparing performance is

inappropriate because this method differs significantly from our task of rotating a block in the hand.

B. Evaluation Metrics and Quantitative Testing

Because it is difficult to analyze the sensations of human operators quantitatively, we designed the following two trajectories using traditional control theory to acquire quantitative data for performance evaluation:

Sinusoidal goal: The torque generated by the feedback device is set to follow the following sinusoidal function:

$$G_s = \alpha \sin(\omega x) \quad (5)$$

where $\alpha = (0.015, 0.030)$ is the amplitude, and $\omega = (8, 16)$ is the frequency. The sinusoidal goal helps measure performance under periodic torque feedback. The following metrics are designed for the Sinusoidal trajectory:

RMSE: The root mean square error is calculated as:

$$RMSE = \sqrt{\frac{1}{n} \sum_{i=1}^n (\varphi_i - G_i)^2} \quad (6)$$

where n is the number of steps, φ_i is the device torque around the Z-axis, G_i is the goal. RMSE evaluates the overall torque feedback accuracy during the telemanipulation process.

Average Latency: The average latency is calculated as:

$$L = \theta_a - \theta_g \quad (7)$$

where θ_a is the phase of the actual torque variation trajectory, θ_g is the phase of the goal torque variation trajectory. Both are obtained from the dominant frequency after the Fourier transform. The average latency evaluates the manipulation delay, a critical measure of real-time feedback capability.

Square wave goal: The torque generated by the feedback device is set to follow the following square wave function:

$$f(x) = \begin{cases} A, & \text{if } ((5t \bmod 2\pi) < \pi) \\ -A, & \text{if } ((5t \bmod 2\pi) \geq \pi) \end{cases} \quad (8)$$

where $A = (0.01, 0.02)$, t is the time variable. The square wave goal helps to evaluate the feedback performance for targets that change in a short time. The following metrics are designed for the step trajectory based on the traditional control theory:

RMSE: The root mean square error is calculated in the same way as the sinusoidal goal.

Overshoot: We calculate the max-percent overshoot:

$$OS = \frac{\varphi_p - G_{step}}{G_{step}} \times 100\% \quad (9)$$

where φ_p is the peak object rotational angle. The overshoot measures the aggressiveness of the Bi-Hap system.

Peak Time: The time required for the response to reach the peak value for the first time, which is denoted by t_p . It indicates how quickly Bi-Hap responds to the torque feedback commands. For all measures, the lower is better.

In the human online test, the following two tasks are designed to evaluate the effectiveness of the Bi-Hap system:

Discrete Angle Test: This test assesses the operator's ability to rotate the object to track a predefined point. The operator is tasked with rotating the object to a randomly specified target angle within a $\pm 1.6^\circ$ range and maintaining that position for 1.6 seconds. Each screen refresh checks whether the object's angle is within the target range; if it is, $S_i = 1$; if not, $S_i = 0$ (i represent the refresh count). The total number of target completions is denoted as S_d :

$$S_d = \sum_{i=1}^n S_i \quad (10)$$

where n represents the total number of refresh counts.

Continuous Angle Test: This test assesses the operator's ability to rotate the object to track a predefined trajectory. Similar to the discrete angle test, the total score increases by one each time the object's angle remains within a $\pm 1.6^\circ$ tolerance of the target trajectory. The total number of target completions is denoted as S_c and it's calculated in the same way as for the discrete angle test.

Subjective survey: After the quantitative evaluation, a subjective human study was conducted to evaluate the effectiveness of the Bi-Hap system in enhancing dexterous telemanipulation. The survey aimed to capture the operators' perceived experience in terms of control accuracy, haptic feedback quality, and overall task performance. Subjects were asked to perform telemanipulation tasks, including discrete angle test and continuous angle test, both with and without the Bi-Hap system. Subjects were selected based on their experience with teleoperation systems, ensuring a range of skill levels was represented. After completing the tasks, each subject completed a survey that assessed their experience across several dimensions, including:

- Q1. To what extent did the Bi-Hap system improve your overall task performance?
- Q2. How clearly could you perceive the torque feedback provided by the Bi-Hap system?
- Q3. To what degree did your precision improve after using the Bi-Hap system?
- Q4. How much did your error correction speed improve after using the Bi-Hap system?
- Q5. How quickly were you able to adapt to using the Bi-Hap system?

Each subject will rate these questions on a scale from 0 to 10, with a post-experiment interview to assess how the Bi-Hap system enhances telemanipulation tasks, particularly regarding user satisfaction and perceived performance.

V. RESULTS AND DISCUSSION

A. Human-Offline Testing

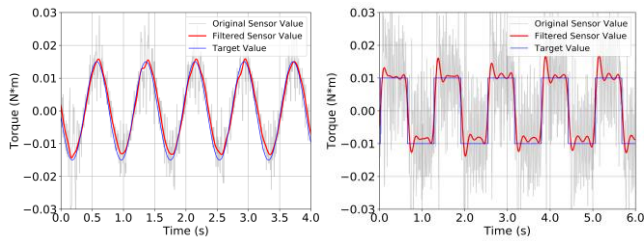
The quantitative testing results for the sinusoidal goal tracking are shown in Table I. Overall, the Bi-Hap can keep a good track of the torque goal with the highest latency of 0.0253s and a maximum root mean square error of 0.0095. More visualized results can be found in the supplementary video. As a comparison, current telemanipulation methods such as MetamorphX [9] need to accelerate their demo 3 times to achieve similar results as ours. The tracking performance deteriorates as the sinusoidal amplitude increases and improves as the sinusoidal frequency decreases, owing to the alteration in task complexity.

TABLE I. SINUSOIDAL GOAL TRACKING PERFORMANCE (5 TESTS)

$\alpha(N \cdot m)$	ω	$RMSE(N \cdot m)$	$L(s)$
0.0150	8	0.0021	0.0126
0.0150	16	0.0058	0.0239
0.0300	8	0.0081	0.0253
0.0300	16	0.0095	0.0174

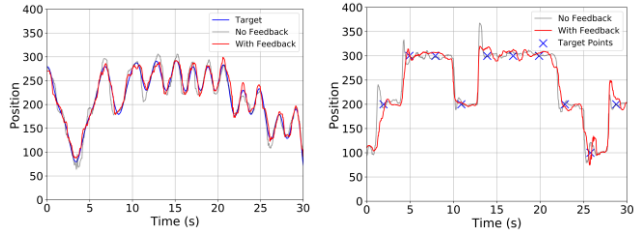
TABLE II. STEP GOAL TRACKING PERFORMANCE (5 TESTS)

$A(N \cdot m)$	$RMSE(N \cdot m)$	$OS(\%)$	$t_p(s)$
0.0100	0.0031	27.38	0.0916
0.0200	0.0144	10.20	0.1800



(a) Sinusoidal goal tracking (b) Square wave goal tracking

Fig. 5. Tracking performance of (a) Sinusoidal Goal and (b) Square wave goal. Both figures show great tracking performance.



(a) Discrete Angle Test (b) Continuous Angle Test

Fig. 6. Test performance of (a) Discrete Angle and (b) Continuous Angle

The results for the step goal tracking are shown in Table II. Different maximum values have varying impacts on the performance of the Bi-Hap system. Since higher output torque leads to greater vibrations, the tracking performance deteriorates as the torque target increases. At the same time, higher target torque requires longer flywheel acceleration, causing a further decline in tracking performance. The opposite is true for overshooting. When the flywheel performance is the same, the effect of correcting torque output remains constant, and the proportion of overshoot decreases as the target torque increases.

Fig. 5 shows the torque variation curves in the sinusoidal and square wave goal tracking tests. Due to sensor noise, we applied a low-pass filter (cut-off frequency of 5Hz, with a filter order of 4) to filter the raw data. The blue curve represents the target torque, the gray curve represents the raw measured data, and the red curve represents the filtered data.

B. Human-Online Testing

In the human-online testing, we invited 5 subjects with telemanipulation experience to conduct the tests, ensuring that each subject was thoroughly familiar with the complete testing environment before the test. Each subject performed five tests across four experimental conditions: discrete, continuous, with feedback, and without feedback. The results are shown in Table III, where A, B, C, D, and E represent the identifiers of the five subjects. The values below each operator in the table represent the average of the five tests for that experimental group. As explained in section IV, we only calculated the average value across these five subjects due to

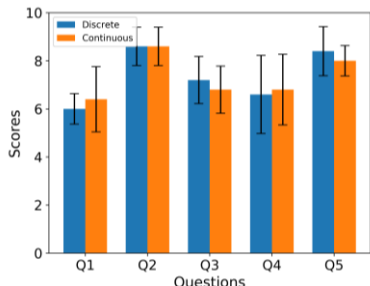


Fig. 7. Average survey results with error bars

TABLE III. REAL-WORLD TESTING IN A TELE-PLAYED GAME (5 TESTS)

Scene	Bi-Hap	A	B	C	D	E	Average
Discrete	Yes	573.4	487.6	592.6	568.6	602.0	586.7
	No	577.0	481.6	558.0	493.6	583.6	566.2
Continuous	Yes	440.8	487.6	558.0	506.0	529.2	504.3
	No	378.2	481.6	517.6	424.4	552.4	470.8

differences in human habits when rotating objects and varying skill levels with the game.

Considering the average score, feedback is better than no feedback. In the discrete task, the average score with feedback is 20.5 higher than without feedback, and in the continuous task, the average score with feedback is 33.5 higher than without feedback. The specific values indicate that the degree of improvement when using the feedback-enabled Bi-Hap system varies among individuals. Observations during the experiment suggest that this variability may be due to differences in tracking strategies and inconsistent operational habits when rotating objects. Nevertheless, the final test scores indicate that the Bi-Hap system with torque feedback can enhance performance in telemanipulation tasks.

To illustrate the Bi-Hap system's impact, we recorded a subject's target manipulation with and without feedback. Figure 6 shows that with feedback (red curve), the subject's manipulation more closely aligns with the target (blue). It can be observed that when tracking rapidly changing targets, the feedback-enabled group adjusts more quickly and has better tracking capability. Additionally, when errors occur, the feedback-enabled group can adjust before the errors become more noticeable, significantly enhancing task performance. Subsequent survey results also confirm this.

C. Survey Results

To analyze user perceptions of the Bi-Hap system, we conducted a questionnaire survey where subjects rated various performance aspects. For question 2, subjects gave the highest ratings in both scenarios, indicating effective torque generation and user perception of the Bi-Hap system, consistent with its low latency and good torque tracking performance. For question 5, the device received the second-highest scores, suggesting good user adaptation, with easier adaptation noted in discrete scenarios due to the game's lower difficulty. For question 3, most users reported improved manipulation accuracy with feedback, especially in discrete target scenarios (see Table 5). For question 4, users believed feedback sped up error correction, though subtle visual feedback differences were less noticeable, leading to corrections only when errors were significant. For question 1, most users saw overall improvement in manipulation performance with feedback. Interviews revealed that feedback was particularly effective for significant changes, while visual cues alone sufficed for minimal changes. Users found feedback beneficial in most scenarios, but excessive feedback could be burdensome in complex situations.

In summary, the Bi-Hap system significantly enhances dexterous telemanipulation by providing effective torque feedback with low latency and precise tracking. Survey results confirm that it improves manipulation accuracy and error correction, particularly in discrete scenarios. Future work will focus on refining feedback adaptability for complex tasks and implementing the Bi-Hap system on real-world robots for further validation and application.

REFERENCES

- [1]. G. Burdea and J. Zhuang, “Dextrous telerobotics with force feedback—An overview part 2: control and implementation,” *Robotica*, vol. 9, no. 3, pp. 291–298, 1991.
- [2]. P. Schleer, M. Vossel, L. Heckmann, S. Drobinsky, L. Theisgen, M. de la Fuente, and K. Radermacher, “Usability of cooperative surgical telemanipulation for bone milling tasks,” *Int. J. Comput. Assist. Radiol. Surg.*, vol. 16, pp. 311–322, 2021.
- [3]. S. Coloma Chacón, “Methods, strategies and application cases for robotic telemanipulation in hazardous environments.” *Industriales*, 2020.
- [4]. M. Panzirsch, A. Pereira, H. Singh, B. Weber, E. Ferreira, A. Gherghescu, L. Hann, E. den Exter, F. van der Hulst, and L. Gerdes, “Exploring planet geology through force-feedback telemanipulation from orbit,” *Sci. Robot.*, vol. 7, no. 65, p. eabl6307, 2022.
- [5]. M. A. Cabrera, J. Tirado, J. Heredia, and D. Tsetserukou, “LinkGlide-S: A wearable multi-contact tactile display aimed at rendering object softness at the palm with impedance control in VR and telemanipulation,” in *2022 IEEE 18th International Conference on Automation Science and Engineering (CASE)*, 2022, pp. 647–652.
- [6]. D. Trinitatova and D. Tsetserukou, “Study of the Effectiveness of a Wearable Haptic Interface With Cutaneous and Vibrotactile Feedback for VR-Based Teleoperation,” *IEEE Trans. Haptics*, vol. 16, no. 4, pp. 463–469, 2023.
- [7]. Y. Park, I. Jo, J. Lee, and J. Bae, “WeHAPTIC: a wearable haptic interface for accurate position tracking and interactive force control,” *Mech. Mach. Theory*, vol. 153, p. 104005, 2020.
- [8]. J. L. Berna Moya, A. van Oosterhout, M. T. Marshall, and D. Martinez Plasencia, “HapticWhirl, a flywheel-gimbal handheld haptic controller for exploring multimodal haptic feedback,” *Sensors*, vol. 24, no. 3, p. 935, 2024.
- [9]. T. Hashimoto, S. Yoshida, and T. Narumi, “Metamorphx: An ungrounded 3-dof moment display that changes its physical properties through rotational impedance control,” in *Proceedings of the 35th Annual ACM Symposium on User Interface Software and Technology*, 2022, pp. 1–14.
- [10]. H. Wang, H. Bai, X. Zhang, Y. Jung, M. Bowman, and L. Tao, “Real-time Dexterous Telemanipulation with an End-Effect-Oriented Learning-based Approach,” *arXiv Prepr. arXiv2408.00853*, 2024.
- [11]. L. Gerini, F. Solari, and M. Chessa, “Passive haptic feedback for more realistic and efficient grasping movements in virtual environments,” in *International Conference on Extended Reality*, 2023, pp. 3–22.
- [12]. Y. Gong, H. Mat Husin, E. Erol, V. Ortenzi, and K. J. Kuchenbecker, “AiroTouch: enhancing telerobotic assembly through naturalistic haptic feedback of tool vibrations,” *Front. Robot. AI*, vol. 11, p. 1355205, 2024.
- [13]. M. Bergholz, M. Ferle, and B. M. Weber, “The benefits of haptic feedback in robot assisted surgery and their moderators: a meta-analysis,” *Sci. Rep.*, vol. 13, no. 1, p. 19215, 2023.
- [14]. A. R. See, J. A. G. Choco, and K. Chandramohan, “Touch, texture and haptic feedback: a review on how we feel the world around us,” *Appl. Sci.*, vol. 12, no. 9, p. 4686, 2022.
- [15]. T. Nakao, K. Kunze, M. Isogai, S. Shimizu, and Y. S. Pai, “FingerFlex: shape memory alloy-based actuation on fingers for kinesthetic haptic feedback,” in *Proceedings of the 19th International Conference on Mobile and Ubiquitous Multimedia*, 2020, pp. 240–244.
- [16]. C. Pacchierotti, D. Prattichizzo, and K. J. Kuchenbecker, “Cutaneous feedback of fingertip deformation and vibration for palpation in robotic surgery,” *IEEE Trans. Biomed. Eng.*, vol. 63, no. 2, pp. 278–287, 2015.
- [17]. H. Alagi, S. E. Navarro, J. Hergenhan, S. Musić, and B. Hein, “Teleoperation with tactile feedback based on a capacitive proximity sensor array,” in *2020 IEEE International Instrumentation and Measurement Technology Conference (I2MTC)*, 2020, pp. 1–6.
- [18]. I. Choi, H. Culbertson, M. R. Miller, A. Olwal, and S. Follmer, “Gravity: A wearable haptic interface for simulating weight and grasping in virtual reality,” in *Proceedings of the 30th Annual ACM Symposium on User Interface Software and Technology*, 2017, pp. 119–130.
- [19]. A. Franzluebbbers and K. Johnsen, “Performance benefits of high-fidelity passive haptic feedback in virtual reality training,” in *Proceedings of the 2018 ACM Symposium on Spatial User Interaction*, 2018, pp. 16–24.
- [20]. B. T. Sterke, K. L. Poggensee, G. M. Ribbers, D. Lemus, and H. Vallery, “Light-weight wearable gyroscopic actuators can modulate balance performance and gait characteristics: A proof-of-concept study,” in *Healthcare*, 2023, vol. 11, no. 21, p. 2841.
- [21]. [1] C. Meijneke, B. Sterke, G. Hermans, W. Gregoor, H. Vallery, and D. Lemus, “Design and evaluation of pint-sized gyroscopic actuators,” in *2021 IEEE/ASME International Conference on Advanced Intelligent Mechatronics (AIM)*, 2021, pp. 454–461.
- [22]. D. Lemus, A. Berry, S. Jabeen, C. Jayaraman, K. Hohl, F. C. T. van der Helm, A. Jayaraman, and H. Vallery, “Controller synthesis and clinical exploration of wearable gyroscopic actuators to support human balance,” *Sci. Rep.*, vol. 10, no. 1, p. 10412, 2020.
- [23]. M. Murer, B. Maurer, H. Huber, I. Aslan, and M. Tscheligi, “Torquescreen: Actuated flywheels for ungrounded kinaesthetic feedback in handheld devices,” in *Proceedings of the Ninth International Conference on Tangible, Embedded, and Embodied Interaction*, 2015, pp. 161–164.
- [24]. T. Tanichi, F. Asada, K. Matsuda, D. Hynds, and K. Minamizawa, “KABUTO: Inducing upper-body movements using a head mounted haptic display with flywheels,” in *SIGGRAPH Asia 2020 Emerging Technologies*, 2020, pp. 1–2.
- [25]. M. Antolini, M. Bordegoni, and U. Cugini, “A haptic direction indicator using the gyro effect,” in *2011 IEEE World Haptics Conference*, 2011, pp. 251–256.
- [26]. X. Jin and J. V. Clark, “GyroCube: A Novice-Friendly Design and Simulation Tool for Gyroscopic Analysis and Optimization of MEMS,” in *ASME International Mechanical Engineering Congress and Exposition*, 2012, vol. 45257, pp. 249–255.
- [27]. <https://www.simplefoc.com/>
- [28]. A. Y. Yousef and S. M. Abdelmaksoud, “Review on field oriented control of induction motor,” *Int. J. Res. Emerg. Sci. Technol. (JREST)*, vol. 2, no. 7, pp. 5–16, 2015.
- [29]. M. Q. Ademola and M. A. Idowu, “THE ADVENT OF THE PROPORTIONAL INTEGRAL DERIVATIVE CONTROLLER: A REVIEW,” *Technology*, vol. 2, p. 10, 2023.
- [30]. P. Song, Y. Yu, and X. Zhang, “Impedance control of robots: an overview,” in *2017 2nd international conference on cybernetics, robotics and control (CRC)*, 2017, pp. 51–55.
- [31]. E. Fernández Cara and E. Zuazua Iriondo, “Control theory: History, mathematical achievements and perspectives,” *Boletín la Soc. Española Matemática Apl.* 26, 79-140., 2003.
- [32]. O. M. Andrychowicz et al., “Learning dexterous in-hand manipulation,” *Int. J. Rob. Res.*, p. 027836491988744, 2019, doi: 10.1177/0278364919887447.
- [33]. M. Plappert et al., “Multi-goal reinforcement learning: Challenging robotics environments and request for research,” *arXiv Prepr. arXiv1802.09464*, 2018